ENGINEERING

Nanotwinned metal MEMS films with unprecedented strength and stability

Gi-Dong Sim,[1] Jessica A. Krogstad,[2] K. Madhav Reddy,[1] Kelvin Y. Xie,[1] Gianna M. Valentino,[1] Timothy P. Weihs,[3] Kevin J. Hemker[1,3]*

Silicon-based microelectromechanical systems (MEMS) sensors have become ubiquitous in consumer-based products, but realization of an interconnected network of MEMS devices that allows components to be remotely monitored and controlled, a concept often described as the "Internet of Things," will require a suite of MEMS materials and properties that are not currently available. We report on the synthesis of metallic nickel-molybdenum-tungsten films with direct current sputter deposition, which results in fully dense crystallographically textured films that are filled with nanotwins. These films exhibit linear elastic mechanical behavior and tensile strengths exceeding 3 GPa, which is unprecedented for materials that are compatible with wafer-level device fabrication processes. The ultrahigh strength is attributed to a combination of solid solution strengthening and the presence of dense nanotwins. These films also have excellent thermal and mechanical stability, high density, and electrical properties that are attractive for next-generation metal MEMS applications.

INTRODUCTION

Microelectromechanical systems (MEMS) have fueled the imagination of engineers and entrepreneurs in recent decades. With repeated technological advances, microsystems have become a multibillion-dollar-per-year industry with numerous consumer-based products that include inertial sensors (accelerometers and gyroscopes), pressure sensors, digital light projectors, mechanical filters, and radiofrequency resonators (*1*, *2*). The application space for MEMS devices can and will be greatly expanded when they can be used in extreme environments and especially at elevated temperatures (*3*), where potential future applications include micropower generation, high-frequency switches and sensors, and digital monitoring and control of residential and commercial components in what is often referred to as the "Internet of Things." These applications demand the development of advanced materials with greater strength, density, electrical and thermal conductivity, dimensional stability, and microscale manufacturability. MEMS materials with this suite of properties are not currently available.

Most commercial MEMS devices still rely on silicon (Si), which cannot be used at elevated temperatures. Significant junction leakage occurs at temperatures above 120°C (*4*), and the mechanical behavior of silicon (brittle at low temperatures and of poor creep strength at elevated temperatures) creates other design problems. Ceramics, such as silicon dioxide (SiO_2), silicon nitride (Si_3N_4), silicon carbide (SiC), and silicon carbon nitride (SiCN), have been developed for MEMS devices that can operate in extreme environments (*3*, *5*, *6*). Some use of these materials has been realized, but wide application has been limited by high residual stresses and the complexity of the fabrication processes. Furthermore, many advanced MEMS applications require materials with both high electrical conductivity and mechanical integrity. Electrodeposited LIGA (a German acronym for lithography, electroplating, and molding) Ni offers a route for microfabrication of metallic parts with high aspect ratios and a more balanced set of properties, but LIGA Ni components have been shown to have highly variable properties that depend on electrodeposition parameters and change rapidly with thermal exposure. Nanocrystalline LIGA Ni has good room temperature yield strength, but instabilities at temperatures as low as 200°C lead to grain growth and a significant loss of strength (*7*). The quest for MEMS materials with high strength and electrical conductivity led us to consider the synthesis of multicomponent Ni alloy films.

RESULTS

In the current study, we fabricated single-phase solid solution nickel-molybdenum-tungsten (Ni-Mo-W) alloy films with an average thickness of 29 μm by means of high-power, direct current (dc) sputter deposition, with a deposition rate of 11.6 μm/hour. The chemistry of the as-deposited films was measured using energy-dispersive spectroscopy (EDS) (fig. S1A) and wavelength-dispersive x-ray spectroscopy (WDS) (Table 1), and the composition of the films was determined to be $Ni_{83.6}Mo_{14}W_{2.4}$ (atomic percent), which exceeds the equilibrium solubility limit of Mo in Ni. Nevertheless, x-ray diffraction (XRD) scans (fig. S1B), transmission electron microscopy (TEM) observations (Fig. 1A), and TEM-based crystal orientation maps (Fig. 1B) indicate that the as-deposited film is a single-phase solid solution alloy. The high energy and quench rates associated with the sputtering process resulted in a preferred (111) out-of-plane crystallographic texture and a far-from-equilibrium supersaturated single-phase microstructure. Similar phenomena have been reported for sputter- and pulse laser–deposited thin films (*8*). The XRD peaks for the solid solution are uniformly shifted as compared to reference Ni peaks, which is attributed to extended lattice spacing due to the incorporation of Mo and W atoms into the Ni lattice.

Cross-sectional focused ion beam (FIB) observations (Fig. 2A) revealed the as-deposited films to have a columnar microstructure as is commonly observed in high–melting temperature materials when sputter-deposited at room temperature (*9*, *10*). The columnar grains were found to be densely packed without intergranular voids, and unexpectedly, cross-sectional TEM images of the as-deposited films (for example, Fig. 2B) revealed an extremely high density of planar crystallographic defects (twins and stacking faults) within the columnar grains. These planar defects are oriented along {111} planes that lie parallel to the film surface and growth direction, and their spacing is extremely fine (1.8 ± 1.1 nm), as illustrated in Fig. 2 (E and F).

[1]Department of Mechanical Engineering, Johns Hopkins University, Baltimore, MD 21218, USA. [2]Department of Materials Science and Engineering, University of Illinois at Urbana-Champaign, Urbana, IL 61801, USA. [3]Department of Materials Science and Engineering, Johns Hopkins University, Baltimore, MD 21218, USA.
*Corresponding author. Email: hemker@jhu.edu

Table 1. Chemical composition, elastic modulus, tensile strength, hardness, and activation volume of the sputter-deposited Ni-Mo-W film obtained from WDS, microtensile, and nanoindentation tests.

Composition (at %)	Elastic modulus (GPa)	Tensile strength (GPa)	Hardness (GPa)			Activation volume (b^3)
			0.05 s^{-1}	0.2 s^{-1}	1 s^{-1}	
$Ni_{83.6\pm0.2}Mo_{14\pm0.2}W_{2.4\pm0.1}$	221 ± 5	2.8 ± 0.3	8.95 ± 0.82	9.1 ± 0.91	9.24 ± 0.86	19.6

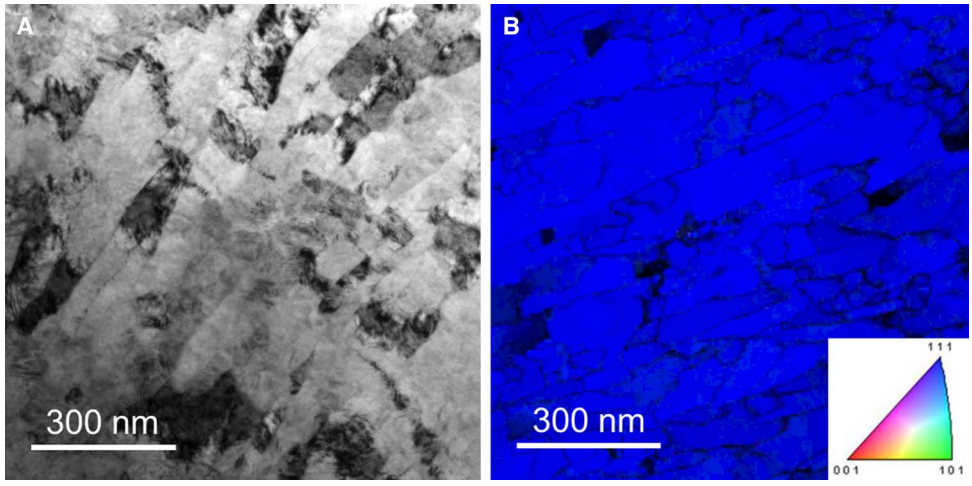

Fig. 1. Plane-view TEM images of the as-deposited film. (**A**) Bright-field plane-view TEM image. (**B**) TEM-based orientation map collected using precession-assisted crystal orientation mapping.

Uniaxial tensile tests were performed on freestanding $Ni_{83.6}Mo_{14}W_{2.4}$ thin films, and the stress-strain response of these sputtered films is compared with literature values of nanoscale metals and other candidate MEMS materials in Fig. 3. Exceptionally high tensile strengths, as high as 3.1 GPa, were measured for the $Ni_{83.6}Mo_{14}W_{2.4}$ films, without any sign of significant plastic deformation. This linear elastic response is highly desirable for MEMS applications, and the overall strength is a significant improvement over pure nanocrystalline Ni (*11*) or binary Ni-W alloys (*12*). The tensile strengths of nanotwinned Cu thin foils with a similar (111) out-of-plane texture (*13*), polysilicon (still one of the most widely used MEMS materials) (*14*), and single-crystal silicon are also much lower than the sputter-deposited $Ni_{83.6}Mo_{14}W_{2.4}$ films. A few materials [for example, nanowhiskers (*15*), Co- and Fe-based metallic glasses (*16*, *17*), and heavily drawn steel wires (*18*)] have been reported to have similar or higher strengths. However, ultrahigh-strength whiskers and wires cannot easily be shaped into MEMS components, and although micromolded bulk metallic glasses hold promise at low temperatures, they will likely not be suitable for elevated temperature applications.

DISCUSSION

The strength of metals and alloys is most effectively tailored by understanding and manipulating the relations between processing, resultant material microstructure, and attendant mechanical properties. The unique microstructural features of the $Ni_{83.6}Mo_{14}W_{2.4}$ films, namely, extended solid solution solubility, textured columnar grains, and finely spaced nanotwins, are directly attributable to their atomic composition and the conditions under which they were deposited. Similarly, the mechanical response of these films can best be understood by quantifying the effect that microstructure has on deformation processes (*19*). Solid solution strengthening can be described using the well-known Fleischer model (*20*) that accounts for dislocation-solute interactions associated with local changes in elastic modulus and atomic spacing. Given the dominant {111} texture of the film and the alignment of the nanotwin boundaries in the plane of the film, dislocations will be forced to bow out and run between twin boundaries in a manner similar to the threading dislocations that have been observed in thin films and multilayered materials (*21*–*23*). Therefore, the strength increase originating from the presence of the nanotwins can be predicted using a confined layer slip (CLS) model (*22*) that has been modified to include the local changes in the lattice parameter and elastic modulus (*8*). Because these dislocation processes act in parallel, the strength of the thin films can be estimated by summing the strengthening mechanisms. The details of this calculation are included in the Supplementary Materials and can be summarized with the following equation

$$\begin{aligned}\sigma_{YS,film} &= \Delta\sigma_{Fleischer} + \Delta\sigma_{Nanotwins} + \Delta\sigma_{Nanotwins,SS} \\ &= 593 + 1972 + 300 = 2865\ MPa\end{aligned} \quad (1)$$

The estimated yield strength is close to the measured tensile strength, and comparison of the various terms indicates that the ultrahigh strength of these films originates primarily from the presence of the nanotwins. The role of the nanotwins has been further confirmed with nanoindentation experiments. The hardness response of the $Ni_{83.6}Mo_{14}W_{2.4}$ films was measured at different indentation strain rates and, like the tensile strength, found to exceed literature values

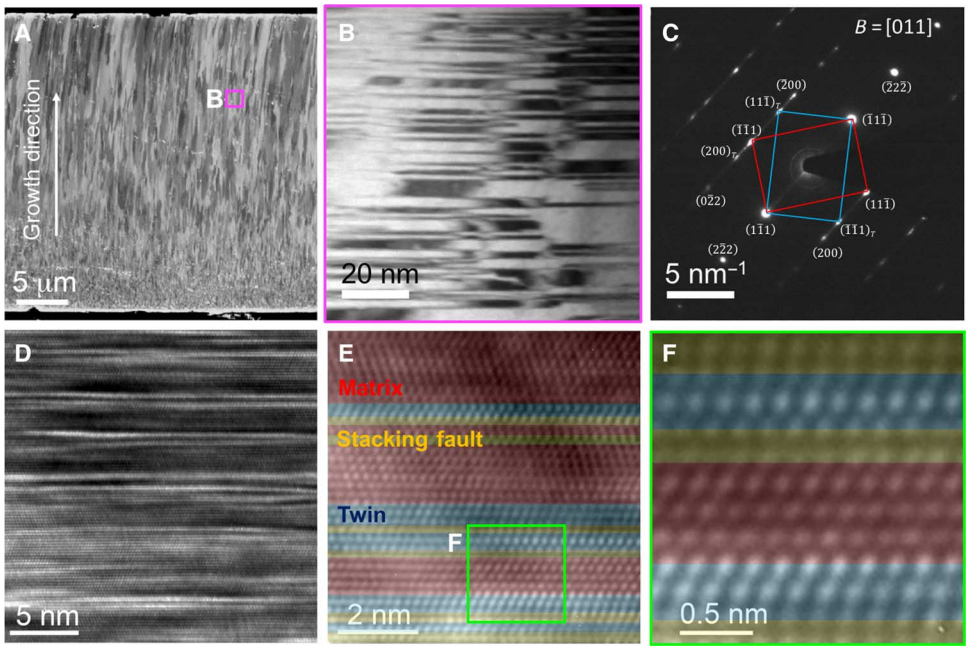

Fig. 2. Cross-sectional microstructure of the as-deposited film. (**A**) Cross-sectional channeling contrast image showing the columnar microstructure of the deposited film. (**B**) Bright-field cross-sectional TEM micrograph. (**C**) Corresponding selected-area electron diffraction pattern indexed for matrix and twin orientations. (**D**) High-resolution TEM (HRTEM) image taken along the [011] zone axis and revealing high-density planar defects. (**E**) HRTEM image showing stacking faults and nanotwin lamellae on {111} planes. (**F**) Magnified view focusing on a few planar defects with better clarity (red, matrix; yellow, stacking fault; blue, twin).

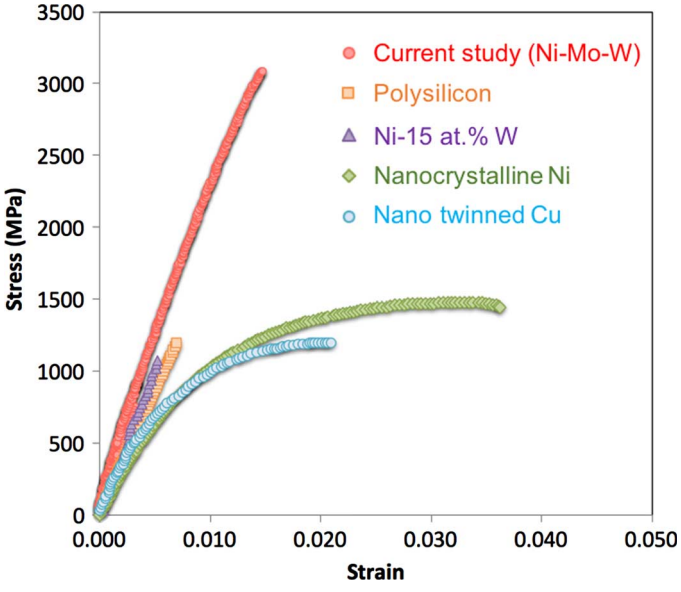

Fig. 3. Tensile stress-strain curves of three Ni-Mo-W thin films from the current study compared with previously reported nanocrystalline Ni (*11*), nanocrystalline Ni-W alloy (*12*), nanotwinned Cu (*13*), and polysilicon thin films (*14*). The linear elastic response and ultrahigh strength are highly desirable for MEMS applications.

for nanocrystalline Ni and nanotwinned Cu (Table 1) (*11*, *13*). Moreover, deformation mechanisms can be characterized by measurements of the activation volumes associated with plastic deformation. Activation volumes for the $Ni_{83.6}Mo_{14}W_{2.4}$ films were obtained from nanoindentation experiments conducted at different indentation rates and determined to be below 0.3 nm^3 (Table 1). This value is orders of magnitude lower than for conventional coarse-grained Ni (~15 nm^3) and entirely consistent with values that have been associated with nanotwinned Cu (*24*) and nanocrystalline metals (*25*).

This is not the first study to call attention to the enhancement of properties offered by nanotwins. Lu *et al.* (*26*) first reported on the synthesis of nanotwinned Cu with ultrahigh strength and excellent electrical conductivity, and their work has motivated others to produce nanotwinned Cu (*13*, *27*, *28*), nanotwinned austenitic stainless steel (*29*), and high-pressure sintered cubic boron nitride (*30*) and diamond (*31*) with nanotwins. The work on sputter-deposited alloys is particularly relevant to the current study, and it is interesting to note that Zhang *et al.* (*32*) reported that the nucleation of nanotwins is promoted by high deposition rates and low stacking fault energies (SFEs). The SFE of Ni is significantly higher than Cu and austenitic stainless steel and appears to preclude the formation of nanotwinned Ni, but alloying with Mo and W has a dual positive effect. In addition to solid solution strengthening, the addition of Mo and W significantly decreases the SFE and promotes nanotwin formation. This point is supported by a recent first-principles study, which concluded that Mo and W are two of the most potent alloying additions (of 26 different elements considered) for reducing the SFE in Ni (*33*). Depositing these Ni-Mo-W alloys with high-power, dc sputter deposition further promoted nanotwinning by both extending the solubility of Mo in Ni and facilitating very high deposition rates. The combination of these effects has allowed us to extend the merits of nanotwinning to high-temperature, Ni-based alloys.

Dimensional stability is particularly important in capacitive-based sensors and guidance MEMS devices, where dimensional changes caused by microstructural evolution or thermal expansion must be significantly less than the expected changes induced during detection/operation of the device. Therefore, thermal and mechanical stability is

a crucial requirement for materials that are to be considered for use in high-temperature MEMS applications. A series of annealing experiments were performed in high vacuum to observe whether the columnar structure and high-density nanotwins are retained after annealing. Figure 4A shows the cumulative area fraction of the in-plane grain size of the film annealed at various temperatures for 1 hour. The film annealed at 600°C did not undergo significant grain growth. TEM cross-sectional images (Fig. 4B) confirmed that the high-density nanotwins were also retained without noticeable change in twin spacing after annealing at 600°C. Only limited grain growth was observed after annealing at 800°C, and extensive grain growth only occurred when the $Ni_{83.6}Mo_{14}W_{2.4}$ films were annealed at 1000°C. FIB channeling contrast and cross-sectional TEM images are given in Fig. 4, C and D, respectively, which show that the columnar grains and high-density nanotwins were retained even after loading up to 3.1 GPa. By comparison, we note that pure nanocrystalline nickel showed significant grain growth and microstructural instability when annealed above 200°C for 1 hour (*34*) and when mechanically loaded up to 1.7 GPa (*35*). The unusual thermal and mechanical stability of the $Ni_{83.6}Mo_{14}W_{2.4}$ films, as compared to nanocrystalline nickel, can be attributed to (i) the presence of nanotwins, which have been reported to have better thermal stability than high-angle grain boundaries (*19*, *27*, *30*), and (ii) the supersaturated single-phase structure. Alloying has been shown to improve stability of nanocrystalline materials, and recent studies indicate that microstructural stability can be correlated to solute enrichment at the grain boundaries (*36*, *37*). In addition to microstructural stability, coefficient of thermal expansion (CTE) measurements have been performed using a custom optical digital image correlation strain measurement technique. The room temperature CTE for the $Ni_{83.6}Mo_{14}W_{2.4}$ films was measured to be $10.7 \times 10^{-6}\ K^{-1}$, which is 22% lower than for pure nickel (*38*).

The electrical resistivity of the $Ni_{83.6}Mo_{14}W_{2.4}$ films measured using a four-point resistivity measurement setup is 111.7 microhm · cm, which is comparable to the 112 microhm · cm measured for electroless plated $Ni_{83.6}Mo_{14.9}P_{1.5}$ films (*39*). It also lies in the same range as bulk nickel-molybdenum alloys (118 to 135 microhm · cm), nickel-chromium alloys (103 to 129 microhm · cm), and nickel-base superalloys (120 to 133 microhm · cm) (*40*). Electrical resistivity of a metallic alloy is governed by electron scattering due to obstacles, such as vacancies, dislocations, grain boundaries, and impurities. The as-deposited films consist of micrometer-scale columnar grains filled with extremely fine nanotwins, but their resistivity is comparable or even lower than coarse-grained nickel alloys. This emphasizes the fact that twin boundaries have a very minor effect on the electrical resistivity while significantly improving the mechanical strength and stability (*26*).

SUMMARY AND CONCLUSIONS

In summary, we fabricated thick (29 μm) thin films of single-phase, solid solution–strengthened $Ni_{83.6}Mo_{14}W_{2.4}$ films by means of high-power, dc sputter deposition. Sputtering Ni with Mo and W that reduced its SFE, at unusually high deposition rates, resulted in the formation of a columnar highly textured and nanotwinned microstructure. The as-deposited films have linear elastic loading, exceptional dimensional stability, and tensile strengths greater than 3 GPa. Deformation models

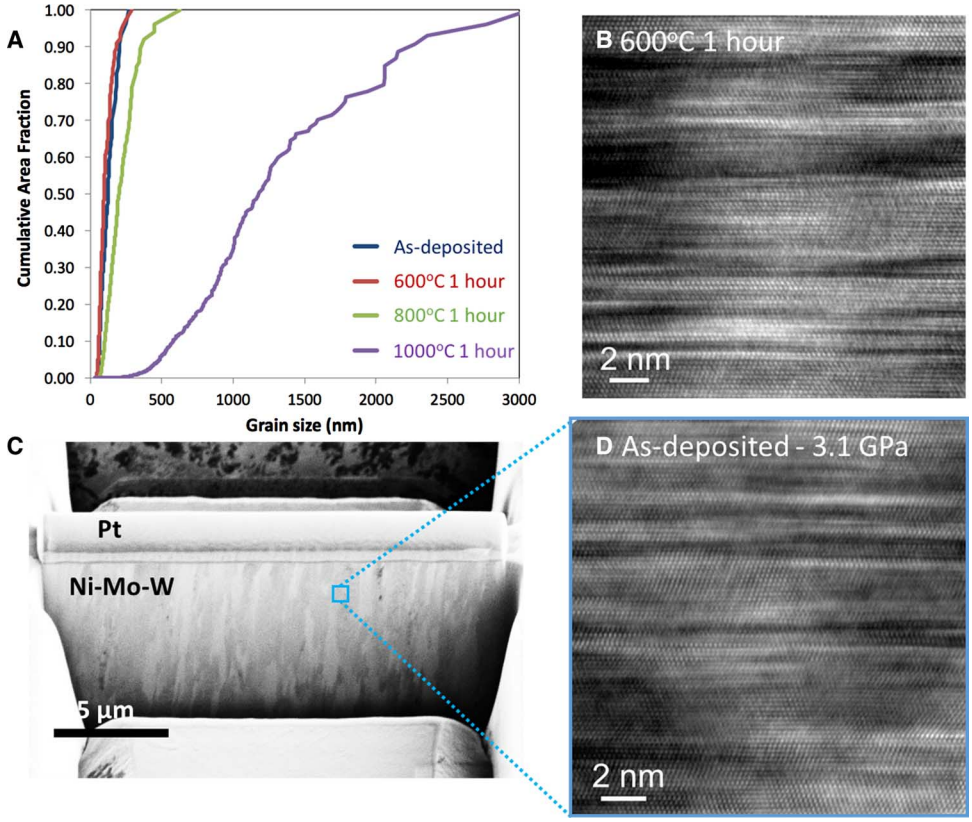

Fig. 4. Excellent thermal and mechanical stability of the $Ni_{83.6}Mo_{14}W_{2.4}$ films. (**A**) Cumulative area fraction of the in-plane grain size of the $Ni_{83.6}Mo_{14}W_{2.4}$ films annealed at various temperatures. (**B**) Cross-sectional TEM image of the film annealed for 1 hour at 600°C. FIB channeling contrast (**C**) and cross-sectional TEM image of a film that was loaded up to 3.1 GPa (**D**). No obvious changes in the columnar microstructure or twin size/spacing were observed.

accredit the primary source of the exceptional strength to the presence of the ultrafine nanotwins. The resultant combination of exceptionally high tensile strength with thermal and mechanical stability points to co-sputtered Ni-Mo-W films as a promising candidate for extending the application envelope for MEMS sensors and components.

MATERIALS AND METHODS

Materials

The Ni-Mo-W thin films were deposited using a custom-built magnetron sputter deposition system with a base pressure of 1×10^{-7} torr. The sputter deposition was used because it is compatible with photolithography-based liftoff and etching techniques that can be used to shape microscale cantilevers and MEMS devices. Films for the current study were sputtered using a dc power of 2500 W and an argon working pressure of 1.0 mtorr for 150 min. The Ar pressure and dc power were carefully chosen to achieve films with low residual stress and ensure a dense microstructure without surface microcracks (*41*). Two targets, Ni–15 at % Mo and Ni–15 at % W, were co-sputtered on a brass substrate to create films with compositional spread, and a relatively molybdenum-rich (compared to tungsten) region was selected for this study. Freestanding thin films were achieved by peeling off the films from the brass substrate and cut into tensile geometries using wire electrical discharge machining. The Ni-Mo-W tensile specimens had an average thickness of 29 μm, gauge widths of 465 μm, and gauge lengths of 1.6 mm.

Methods

The chemistry of the as-deposited films was measured using energy-dispersive spectroscopy in a CM300 TEM (fig. S1A) and wavelength-dispersive x-ray spectroscopy in JEOL 8600 SuperProbe, with pure Ni, Mo, and W crystals serving as standards. Operating conditions for WDS included a 40° takeoff angle, a beam energy of 20 keV, a beam current of 40 nA, and a beam diameter of 2 μm. Sixteen point measurements were made at different regions of the film, and the average chemical composition of the alloy was determined to be $Ni_{83.6}Mo_{14}W_{2.4}$ (atomic percent). A Struers twin-jet electropolisher and an electrolyte of 15 volume % perchloric acid and 85 volume % ethanol were used for in-plane TEM sample preparation, and FIB (FEI Strata DB235) lift-out was used to obtain cross-sectional TEM foils. TEM images were acquired using a Philips CM300 microscope at 300 kV. The crystal orientation of the films was assessed using XRD and further confirmed using TEM orientation mapping technique based on collection of automated crystal orientation mapping.

SUPPLEMENTARY MATERIALS

Supplementary material for this article is available at http://advances.sciencemag.org/cgi/content/full/3/6/e1700685/DC1
Supplementary Materials and Methods
Supplementary Text
fig. S1. Scanning electron microscopy–EDS and XRD graph of the Ni-Mo-W film.
fig. S2. Yield strength predicted from the CLS model.
References (*42*–*57*)

REFERENCES AND NOTES

1. S. E. Lyshevski, *MEMS and NEMS: Systems, Devices, and Structures* (CRC Press, 2002).
2. C. T. Leondes, *MEMS/NEMS Handbook Techniques and Applications* (Springer, 2006).
3. J. A. Krogstad, C. Keimel, K. J. Hemker, Emerging materials for microelectromechanical systems at elevated temperatures. *J. Mater. Res.* **29**, 1597–1608 (2014).
4. P. G. Neudeck, R. S. Okojie, L.-Y. Chen, High-temperature electronics—A role for wide bandgap semiconductors? *Proc. IEEE* **90**, 1065–1076 (2002).
5. L. A. Liew, W. G. Zhang, L. N. An, S. Shah, R. L. Luo, Y. P. Liu, T. Cross, M. L. Dunn, V. Bright, J. W. Daily, R. Raj, K. Anseth, Ceramic MEMS—New materials, innovative processing and future applications. *Am. Ceram. Soc. Bull.* **80**, 25–30 (2001).
6. L. Jiang, R. Cheung, A review of silicon carbide development in MEMS applications. *Int. J. Comput. Mater. Sci. Surf. Eng.* **2**, 227–242 (2009).
7. H. S. Cho, K. J. Hemker, K. Lian, J. Goettert, G. Dirras, Measured mechanical properties of LIGA Ni structures. *Sensor. Actuat. A Phys.* **103**, 59–63 (2003).
8. T. J. Rupert, J. C. Trenkle, C. A. Schuh, Enhanced solid solution effects on the strength of nanocrystalline alloys. *Acta Mater.* **59**, 1619–1631 (2011).
9. J. A. Thornton, Influence of apparatus geometry and deposition conditions on the structure and topography of thick sputtered coatings. *J. Vac. Sci. Technol.* **11**, 666–670 (1974).
10. J. W. Patten, Columnar grain-structure in thick sputtered nickel. *Thin Solid Films* **75**, 205–211 (1981).
11. R. Schwaiger, B. Moser, M. Dao, N. Chollacoop, S. Suresh, Some critical experiments on the strain-rate sensitivity of nanocrystalline nickel. *Acta Mater.* **51**, 5159–5172 (2003).
12. S. J. Suresha, M. Haj-Taieb, K. Bade, J. Aktaa, K. J. Hemker, The influence of tungsten on the thermal stability and mechanical behavior of electrodeposited nickel MEMS structures. *Scr. Mater.* **63**, 1141–1144 (2010).
13. X. Zhang, H. Wang, X. H. Chen, L. Lu, K. Lu, High-strength sputter-deposited Cu foils with preferred orientation of nanoscale growth twins. *Appl. Phys. Lett.* **88**, 173116 (2006).
14. W. N. Sharpe Jr., Murray lecture tensile testing at the micrometer scale: Opportunities in experimental mechanics. *Exp. Mech.* **43**, 228–237 (2003).
15. G. Richter, K. Hillerich, D. S. Gianola, R. Mönig, O. Kraft, C. A. Volkert, Ultrahigh strength single crystalline nanowhiskers grown by physical vapor deposition. *Nano Lett.* **9**, 3048–3052 (2009).
16. A. Inoue, B. L. Shen, H. Koshiba, H. Kato, A. R. Yavari, Cobalt-based bulk glassy alloy with ultrahigh strength and soft magnetic properties. *Nat. Mater.* **2**, 661–663 (2003).
17. A. Makino, T. Kubota, C. Chang, M. Makabe, A. Inoue, FeSiBP bulk metallic glasses with unusual combination of high magnetization and high glass-forming ability. *Mater. Trans.* **48**, 3024–3027 (2007).
18. Y. Tomota, T. Suzuki, A. Kanie, Y. Shiota, M. Uno, A. Moria, N. Minakawa, Y. Morii, In situ neutron diffraction of heavily drawn steel wires with ultra-high strength under tensile loading. *Acta Mater.* **53**, 463–467 (2005).
19. K. Lu, L. Lu, S. Suresh, Strengthening materials by engineering coherent internal boundaries at the nanoscale. *Science* **324**, 349–352 (2009).
20. R. L. Fleischer, The strengthening of metals, in *Solid-Solution Hardening*. D. Peckner, Ed. (Reinhold Publishing Corp., 1964).
21. W. D. Nix, Mechanical properties of thin films. *Metall. Trans. A* **20**, 2217–2245 (1989).
22. A. Misra, J. P. Hirth, R. G. Hoagland, Length-scale-dependent deformation mechanisms in incoherent metallic multilayered composites. *Acta Mater.* **53**, 4817–4824 (2005).
23. Z. S. You, X. Li, L. Gui, Q. Lu, T. Zhu, H. Gao, L. Lu, Plastic anisotropy and associated deformation mechanisms in nanotwinned metals. *Acta Mater.* **61**, 217–227 (2013).
24. L. Lu, R. Schwaiger, Z. W. Shan, M. Dao, K. Lu, S. Suresh, Nano-sized twins induce high rate sensitivity of flow stress in pure copper. *Acta Mater.* **53**, 2169–2179 (2005).
25. R. J. Asaro, S. Suresh, Mechanistic models for the activation volume and rate sensitivity in metals with nanocrystalline grains and nano-scale twins. *Acta Mater.* **53**, 3369–3382 (2005).
26. L. Lu, Y. F. Shen, X. H. Chen, L. H. Qian, K. Lu, Ultrahigh strength and high electrical conductivity in copper. *Science* **304**, 422–426 (2004).
27. O. Anderoglu, A. Misra, H. Wang, X. Zhang, Thermal stability of sputtered Cu films with nanoscale growth twins. *J. Appl. Phys.* **103**, 094322 (2008).
28. L. Lu, X. Chen, X. Huang, K. Lu, Revealing the maximum strength in nanotwinned copper. *Science* **323**, 607–610 (2009).
29. X. Zhang, A. Misra, H. Wang, M. Nastasi, J. D. Embury, T. E. Mitchell, R. G. Hoagland, J. P. Hirth, Nanoscale-twinning-induced strengthening in austenitic stainless steel thin films. *Appl. Phys. Lett.* **84**, 1096–1098 (2004).
30. Y. J. Tian, B. Xu, D. Yu, Y. Ma, Y. Wang, Y. Jiang, W. Hu, C. Tang, Y. Gao, K. Luo, Z. Zhao, L.-M. Wang, B. Wen, J. He, Z. Liu, Ultrahard nanotwinned cubic boron nitride. *Nature* **493**, 385–388 (2013).
31. Q. Huang, D. Yu, B. Xu, W. Hu, Y. Ma, Y. Wang, Z. Zhao, B. Wen, J. He, Z. Liu, Y. Tian, Nanotwinned diamond with unprecedented hardness and stability. *Nature* **510**, 250–253 (2014).
32. X. Zhang, A. Misra, H. Wang, T. D. Shen, M. Nastasi, T. E. Mitchell, J. P. Hirth, R. G. Hoagland, J. D. Embury, Enhanced hardening in Cu/330 stainless steel multilayers by nanoscale twinning. *Acta Mater.* **52**, 995–1002 (2004).
33. S. L. Shang, C. L. Zacherl, H. Z. Fang, Y. Wang, Y. Du, Z. K. Liu, Effects of alloying element and temperature on the stacking fault energies of dilute Ni-base superalloys. *J. Phys. Condens. Matter* **24**, 505403 (2012).

34. M. Thuvander, M. Abraham, A. Cerezo, G. D. W. Smith, Thermal stability of electrodeposited nanocrystalline nickel and iron–nickel alloys. *Mater. Sci. Technol.* **17**, 961–970 (2001).
35. B. Wang, M. T. Alam, M. A. Haque, Grain growth in nanocrystalline nickel films at low temperature and stress. *Scr. Mater.* **71**, 1–4 (2014).
36. A. J. Detor, C. A. Schuh, Tailoring and patterning the grain size of nanocrystalline alloys. *Acta Mater.* **55**, 371–379 (2007).
37. F. Tang, D. S. Gianola, M. P. Moody, K. J. Hemker, J. M. Cairney, Observations of grain boundary impurities in nanocrystalline Al and their influence on micro structural stability and mechanical behaviour. *Acta Mater.* **60**, 1038–1047 (2012).
38. A. S. Pavlovic, V. S. Babu, M. S. Seehra, High-temperature thermal expansion of binary alloys of Ni with Cr, Mo and Re: A comparison with molecular dynamics simulations. *J. Phys. Condens. Matter* **8**, 3139–3149 (1996).
39. I. Koiwa, M. Usuda, K. Yamada, T. Osaka, Effect of heat-treatment on properties of electroless-deposited nickel-molybdenum-phosphorus alloy-films. *J. Electrochem. Soc.* **135**, 718–726 (1988).
40. J. L. Everhart, *Engineering Properties of Nickel and Nickel Alloys* (Springer, 1971), 229 pp.
41. D. E. Burns, Y. Zhang, T. P. Weihs, K. J. Hemker, Properties of sputter deposited Ni-base superalloys for microelectromechanical systems. *Thin Solid Films* **558**, 20–23 (2014).
42. W. C. Oliver, G. M. Pharr, Measurement of hardness and elastic modulus by instrumented indentation: Advances in understanding and refinements to methodology. *J. Mater. Res.* **19**, 3–20 (2004).
43. H. M. Ledbetter, R. P. Reed, Elastic properties of metals and alloys, I. Iron, nickel, and iron-nickel alloys. *J. Phys. Chem. Ref. Data* **2**, 531–618 (1973).
44. Y. Mishima, S. Ochiai, N. Hamao, M. Yodogawa, T. Suzuki, Solid solution hardening of nickel—Role of transition metal and B-subgroup solutes. *Trans. Jpn. Inst. Met.* **27**, 656–664 (1986).
45. H. B. Huang, F. Spaepen, Tensile testing of free-standing Cu, Ag and Al thin films and Ag/Cu multilayers. *Acta Mater.* **48**, 3261–3269 (2000).
46. M. A. Haque, M. T. A. Saif, Deformation mechanisms in free-standing nanoscale thin films: A quantitative in situ transmission electron microscope study. *Proc. Natl. Acad. Sci. U.S.A.* **101**, 6335–6340 (2004).
47. W. N. Sharpe Jr., J. Pulskamp, B. G. Mendis, C. Eberl, D. S. Gianola, R. Polcawich, K. J. Hemker, Tensile stress-strain curves of gold film, in *ASME 2006 International Mechanical Engineering Congress and Exposition Materials, Nondestructive Evaluation, and Pressure Vessels and Piping* (ASME, 2007), pp. 533–540.
48. G.-D. Sim, Y. S. Choi, D. Lee, K. H. Oh, J. J. Vlassak, High tensile strength of sputter-deposited ZrB_2 ceramic thin films measured up to 1016 K. *Acta Mater.* **113**, 32–40 (2016).
49. Y. M. Wang, A. V. Hamza, E. Ma, Temperature-dependent strain rate sensitivity and activation volume of nanocrystalline Ni. *Acta Mater.* **54**, 2715–2726 (2006).
50. W. F. Hosford, *The Mechanics of Crystals and Textured Polycrystals* (Oxford Univ. Press, 1993), 248 pp.
51. T. H. Courtney, *Mechanical Behavior of Materials* (McGraw Hill, ed. 2, 2000), 733 pp.
52. C. A. Schuh, T. G. Nieh, H. Iwasaki, The effect of solid solution W additions on the mechanical properties of nanocrystalline Ni. *Acta Mater.* **51**, 431–443 (2003).
53. E. O. Hall, The deformation and ageing of mild steel: III. Discussion of results. *Proc. Phys. Soc. B* **64**, 747 (1951).
54. N. J. Petch, The cleavage strength of polycrystals. *J. Iron Steel Inst.* **174**, 25–28 (1953).
55. Z. S. You, L. Lu, K. Lu, Tensile behavior of columnar grained Cu with preferentially oriented nanoscale twins. *Acta Mater.* **59**, 6927–6937 (2011).
56. Q. H. Bui, G. Dirras, S. Ramtani, J. Gubicza, On the strengthening behavior of ultrafine-grained nickel processed from nanopowders. *Mater. Sci. Eng. A* **527**, 3227–3235 (2010).
57. Z. Yang, J. L. Wang, Orientation-dependent hardness in as-deposited and low-temperature annealed Ti/Ni multilayer thin films. *J. Appl. Mech.* **82**, 011008 (2015).

Acknowledgments: We thank C. Keimel (General Electric Global Research) for fruitful discussions and K. Livi and S. Dasgupta for help with chemical analysis and orientation mapping. **Funding:** This work was supported by the NSF under grant GOALI DMR-1410301.
Author contributions: J.A.K. and K.J.H. proposed the study, and J.A.K. sputter-deposited the films under the supervision of T.P.W. G.-D.S. conducted mechanical experiments; G.-D.S., K.M.R., and K.Y.X., conducted chemical and microstructural characterization; and G.M.V. measured the physical properties of the films, all under the supervision of K.J.H. All authors analyzed the data and discussed the results, and G.-D.S. and K.J.H. wrote the manuscript with reviews and input from all authors. **Competing interests:** G.-D.S., J.A.K., G.M.V., T.P.W., and K.J.H. are authors on a U.S. provisional patent application related to this work, filed by Johns Hopkins Technology Ventures (application no. 62/492,558, filed 1 May 2017). All other authors declare that they have no competing interests. **Data and materials availability:** All data needed to evaluate the conclusions in the paper are present in the paper and/or the Supplementary Materials. Additional data related to this paper may be requested from the authors.

Submitted 6 March 2017
Accepted 11 May 2017
Published 28 June 2017
10.1126/sciadv.1700685

Citation: G.-D. Sim, J. A. Krogstad, K. M. Reddy, K. Y. Xie, G. M. Valentino, T. P. Weihs, K. J. Hemker, Nanotwinned metal MEMS films with unprecedented strength and stability. *Sci. Adv.* **3**, e1700685 (2017).

Science Advances

Nanotwinned metal MEMS films with unprecedented strength and stability

Gi-Dong Sim, Jessica A. Krogstad, K. Madhav Reddy, Kelvin Y. Xie, Gianna M. Valentino, Timothy P. Weihs and Kevin J. Hemker

Sci Adv **3** (6), e1700685.
DOI: 10.1126/sciadv.1700685